TOKYO METROPOLITAN UNIVERSITY
東京都立大学

The Seventh
INTERNATIONAL CONFERENCE ON
TETHERS in SPACE
Hosted by York University, Toronto, Canada
June 2-5, 2024

Numerical and Experimental Study on Effect of Net-bullet Ejection Angles and Initial Distances on Successful Space-Debris Capture

Andry Renaldy Pandie, Prof. Hirohisa Kojima, and A. Puente-Flores

Agenda:

1. Background
2. Research objectives
3. Methodology
4. Result
5. Conclusions

1. Background

- Space debris speeds in LEO: 8.33 to 15 km/s. [1, 2].
- Increasing debris collisions heighten space debris threat: 4-5 objects yearly [3].
- ADR works best because: focusing on high-mass, high-probability, high-altitude objects [5].

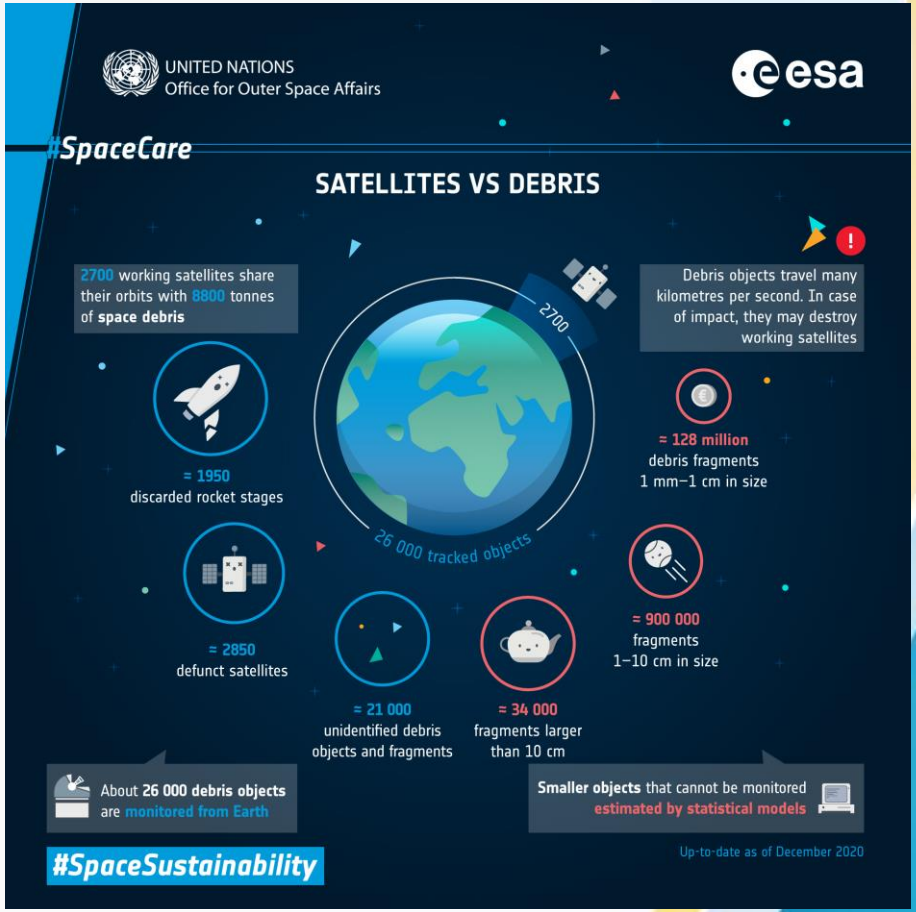

Fig. 1 The spread of space debris [4]

[1] C. P. Mark, S. Kamath, Review of active space debris removal methods, Space Policy 47 (2019) 194–206.
[2] W. Gołębiowski, R. Michalczyk, M. Dyrek, U. Battista, K. Wormnes, Validated simulator for space debris removal with nets and other flexible tethers applications, Acta Astronautica 129 (2016) 229–240.
[3] M. Maestrini, P. Di Lizia, Guidance strategy for autonomous inspection of unknown non-cooperative resident space objects, Journal of Guidance, Control, and Dynamics 45 (6) (2022) 1126–1136.
[4] ESA, Satellites vs debris (https://www.esa.int/ESA_Multimedia/Images/2021/02/Satellites_vs_Debris).
[5] K. Wormnes, R. Le Letty, L. Summerer, R. Schonenborg, O. Dubois-matra, et. al., ESA technologies for space debris remediation, in: Proceedings of the 6th European Conference on Space Debris, Darmstadt, 2013

Tether net

The tether net is one of a promising ADR method, because: [6, 7]

- capture and removal mechanism
- trajectory motion capabilities
- effectiveness in targeting debris
- performance characteristics

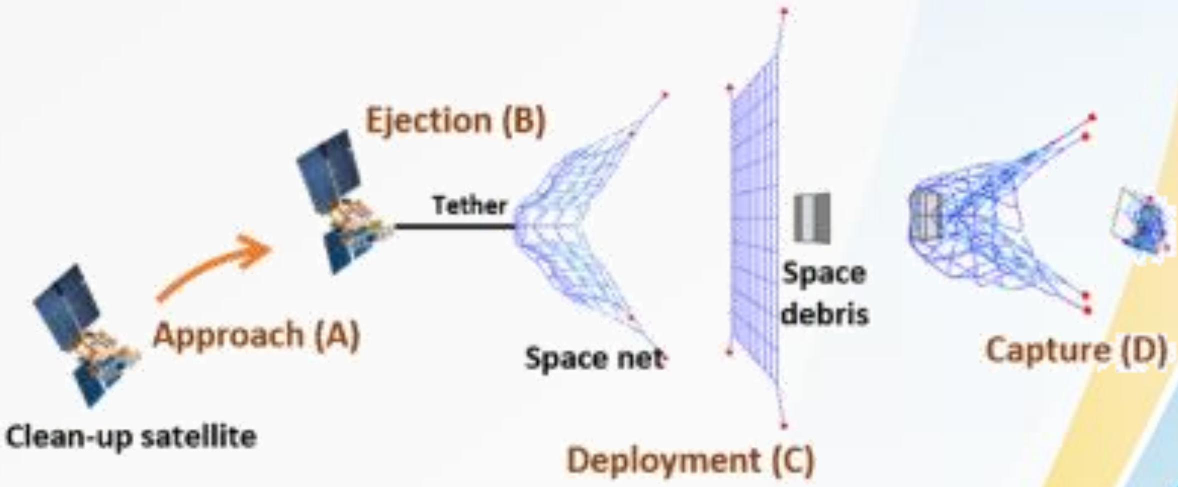

Fig. 2 Stages of net to capture space debris [8]

[6] M. Shan, J. Guo, E. Gill, Deployment dynamics of tethered-net for space debris removal, Acta Astronautica220 132 (2017) 293–302
[7] G. Zhang, Q. Zhang, Z. Feng, Q. Chen, T. Yang, A simplified model for fast analysis of the deployment dynamics of tethered-net in space, Advances in Space Research 68 (4) (2021) 1960–1974
[8] H. Shin, M. Jang, U. Hwang, et al., Capture simulation using space-nets for space debris in various motions, International Journal of Aeronautical and Space Sciences 23 (2023) 2093–2480

Potential gaps from existing studies

- not address the specific impact of net-bullet ejection angles and initial distances on successful space-debris capture [9, 10, 11, 12].

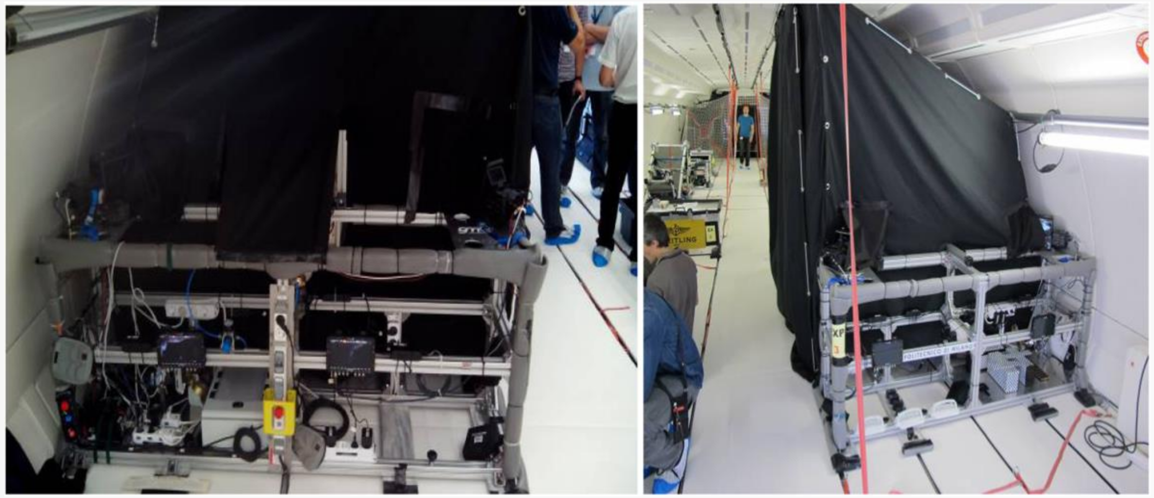

a) Rack holding for the net and mockup debris launching system

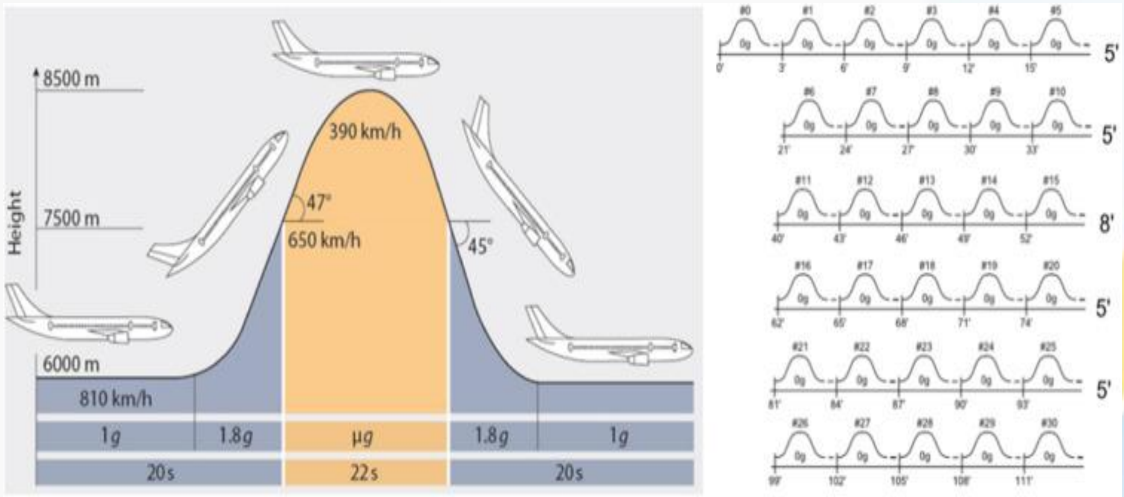

b) Flight profile

Fig. 3 Medina's experiment set up [12]

[9] I. Sharf, B. Thomsen, E. M. Botta, A. K. Misra, Experiments and simulation of a net closing mechanism for tether-net capture of space debris, Acta Astronautica 139 (2017) 332–343.
[10] S. Yue, M. Li, Z. Zhao, Z. Du, C. Wu, Q. Zhang, Parameter analysis and experiment validation of deployment characteristics of a rectangular tether-net, Aerospace 10 (2) (2023) 1–21.
[11] Y. Yang, W. Hu, Z. Liu, Configuration design and collision dynamics analysis of flexible nets for space debris removal, Acta Astronautica 211 (2023) 249–256.
[12] A. Medina, L. Cercós, R. M. Stefanescu, R. Benvenuto, et.al., Validation results of satellite mock-up capturing experiment using nets, Acta Astronautica 134 (2017) 314–332.

2. Research objectives

- the impact of net-bullet ejection angles
- the influence of initial distances
- integrate numerical simulations and practical experiments

to contact & capture condition

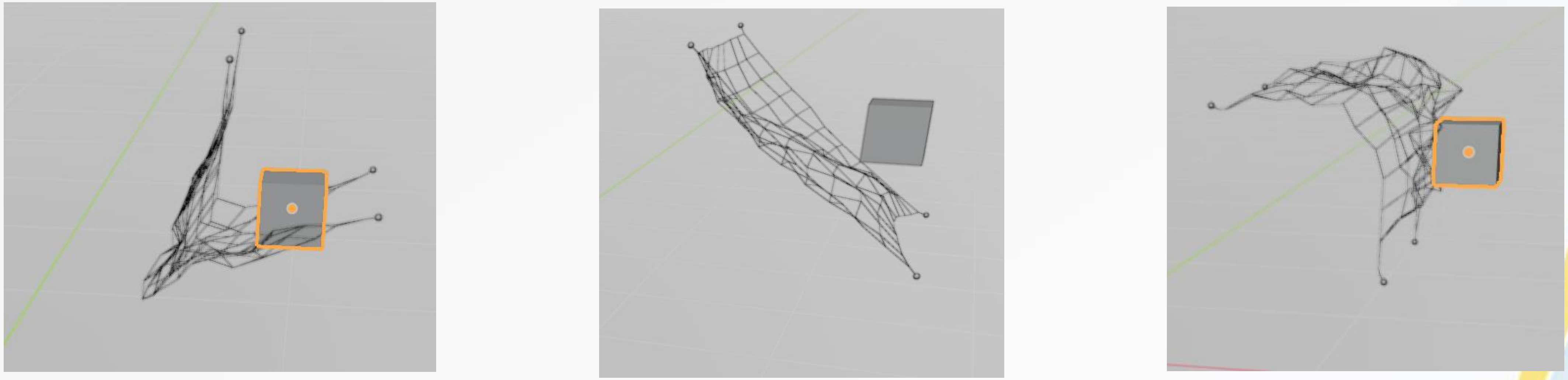

a) Before full deployment b) Full deployment c) Start to shrink

Fig. 4 Projection of net condition just before contact

3. Methodology

Table 1. Simulation and experiment specifications

Parameter	Value
Amount of bullets (CM)	4
Bullet ejection angle (θ)	15, 30, 45°
Shooting speed of bullet (v_b)	10.02 m/s
Net mass + total mass of bullets	8.8 + 21.6 g
Shooting angle of net (φ)	45°
Net side length (L_{net})	1 m
Thread length to attaching bullet to the net (L_{CT})	5 cm
Net height from the ground (y_{0_n})	129.4 m
Initial distance between net and debris (D_{init})	1, 1.5, 2, 2.5, 3 m
Debris side length (L_d)	10 cm
Debris mass (m_d)	150 g
Motion of debris ejection	vertical upward

Numerical simulation:

- Software tools: Python Spyder, Blender, and DippMotion.

Ground test:

- Net material: Kevlar.
- Mockup debris: 3D-printed plastic.
- Setup: calibrated spring-based net launcher with CM for precise angle ejection.
- Data collection: high-speed cameras (DITECT HAS-D72)

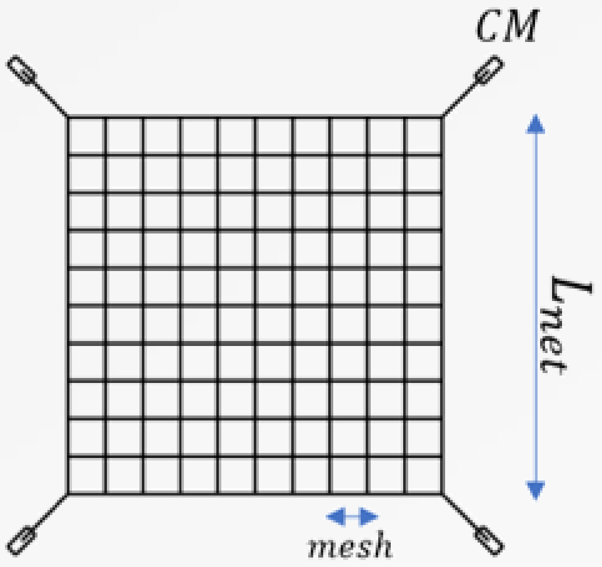

Fig. 5 Design of net

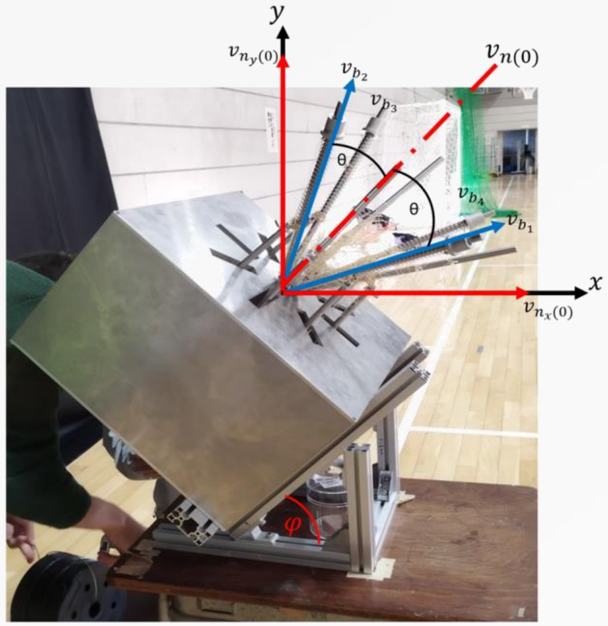

Fig. 6 Ejector mechanism of net

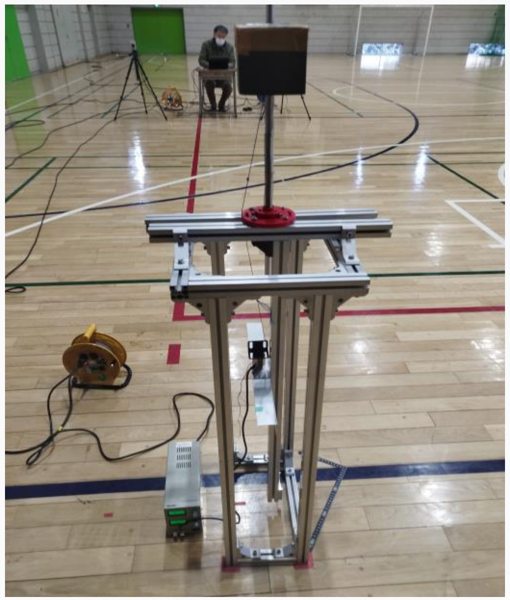
Fig. 7 Ejector mechanism of mockup debris

Fig. 8 Set up of the experiment

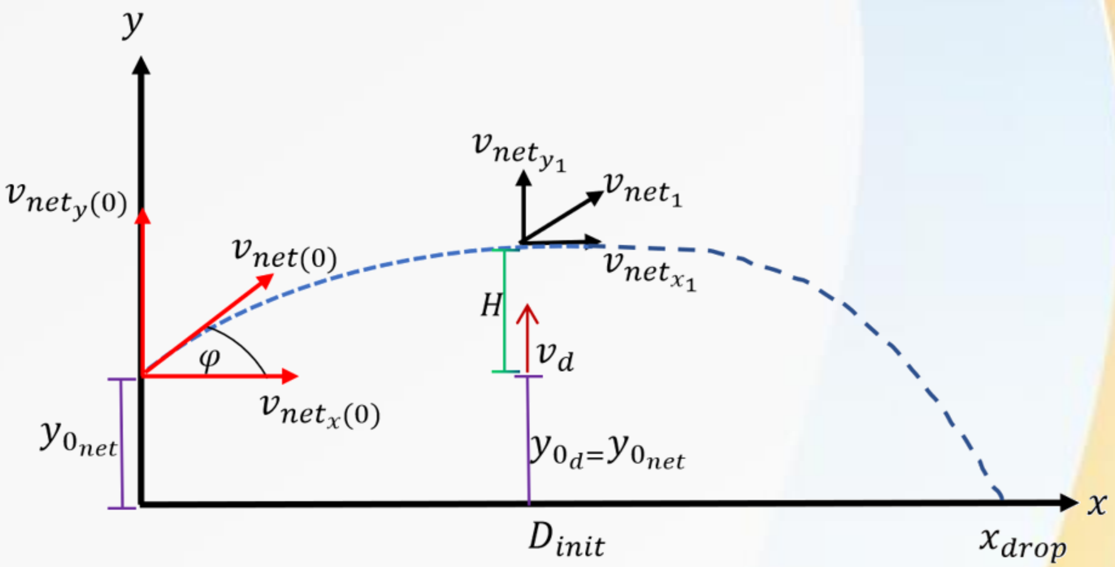

Fig. 9 Projection of net and debris motion

- The analysis process: tracking the speed and range of the net and debris based on parabolic equations and upward vertical motion.
- Time history of net perimeter: using the polyarea function in MATLAB.

Table 2. Spring configuration on a net ejector mechanism

Parameter	Value
Spring constant (k_1)	231 N/m
Length of spring	15 cm
Spring compression (Δx_1)	10 cm

shooting speed of bullet →

$$v_b = \Delta x_1 \sqrt{\frac{k_1}{m_{CM}}} \quad (1)$$

shooting speed of net →

$$v_{net(0)} = v_b \cos\theta \quad (2)$$

Table 3. Spring configuration on a debris ejector mechanism

Parameter	Value
Spring constant (k_2)	77 N/m
Length of spring	45 cm
Spring compression (Δx_2)	must be adjusted

shooting speed of debris →

$$v_d = \Delta x_2 \sqrt{\frac{k_2}{m_d}} \quad (3)$$

Parabolic motion equation of net

- The reference variables for collision points: $H_{d_{max}}$ and H_{net}

time to reach Fig. 10(b):

$$t_{y_{full}} = \frac{\sqrt{2}L_{net}}{2v_b \sin\theta} \quad (4)$$

the height of the net in this condition is given as:

$$H_{net} = y_{0_{net}} + D_{init}\tan\varphi - \frac{1}{2}gt_{y_{full}}^2 \quad (5)$$

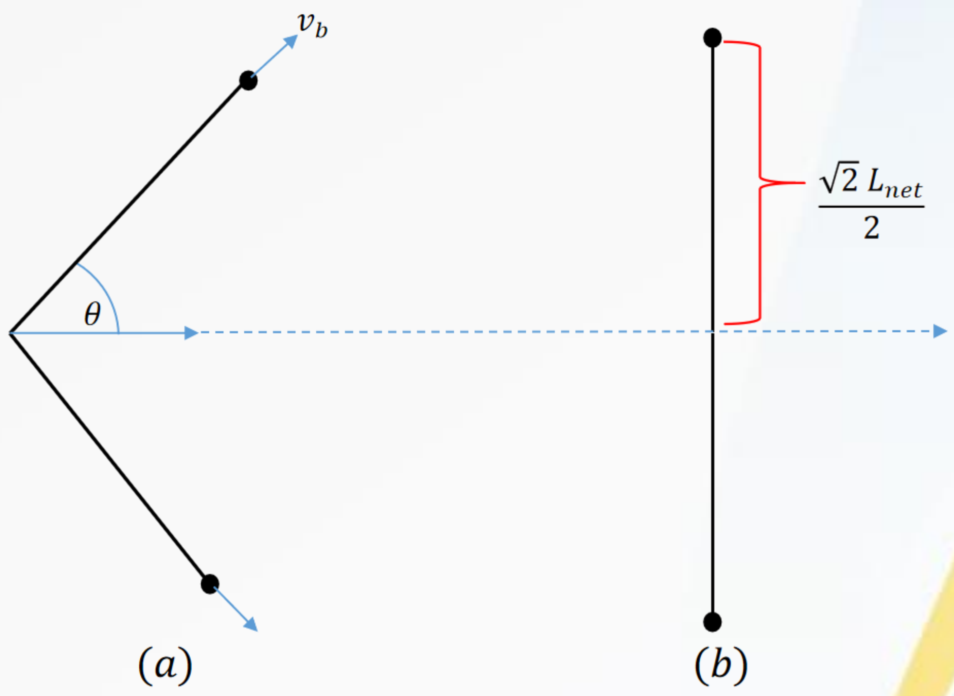

Fig. 10 Projection of net condition: initial condition (a) full deployment (b)

Evaluating the performance of net deployment

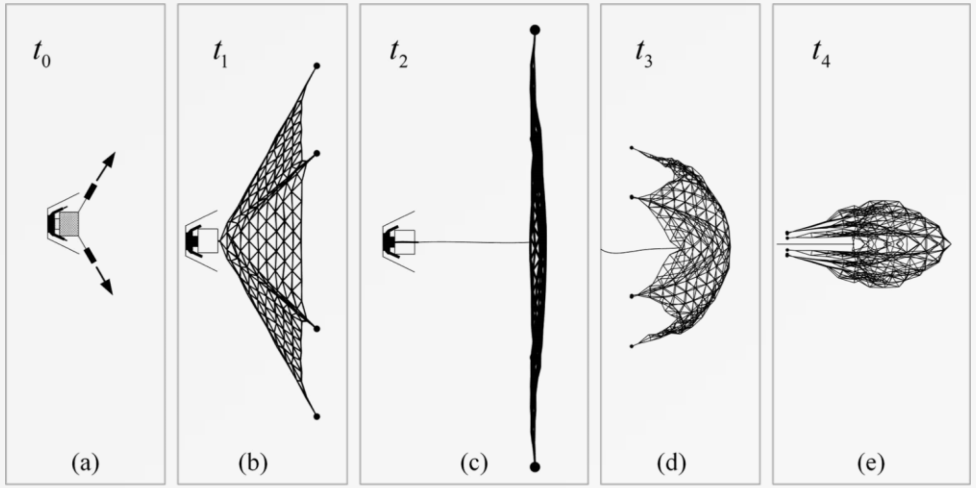

Fig. 11 Stages of ejection cycle of tether net [13]

$$\alpha = \frac{n_b m_d}{m_{net}} \quad (6)$$

$$t_{pullout} = t_1 = \frac{\frac{L_{net}}{2}}{v_b}\left(1 + \frac{1}{2\alpha}\right) \quad (7)$$

$$v_{pullout} = \frac{v_b}{\sqrt{1 + \frac{1}{\alpha}\left(2 + \frac{1}{\alpha}\right)}} \quad (8)$$

[14]

$$t_{contact} = t_{pullout} + \frac{D_{init} + (v_d t_{pullout}) - \frac{1}{4} L_{net} \cos\theta}{v_{pullout} - v_d} \quad (9)$$

[13] G. Zhang, Q. Zhang, Z. Feng, Q. Chen, T. Yang, A simplified model for fast analysis of the deployment dynamics of tethered-net in space, Advances in Space Research 68 (4) (2021) 1960–1974.

[14] A. R. Pandie, H. Kojima, Allowable initial relative velocity of a net to contact and capture space debris, Trans. JSASS Aerospace Tech. Japan 21 (2023) 45–54.

Vertical upward motion of debris

$$H_{d_{max}} = \frac{\frac{1}{2}k_2 \Delta x_2^2}{m_d g} = \frac{\frac{1}{2}v_d^2}{g} \qquad (10)$$

Because x_d is varied and we have correlated with the net, as shown in Eq. (4), we assume that $H_{d_{max}} = H_{net(x)}$

Thus, the spring on the debris ejector mechanism needs to be compressed:

$$\Delta x_2 = \sqrt{\frac{m_d v_d^2}{k_2}} = \sqrt{\frac{2H_{d_{max}} m_d g}{k_2}} \qquad (11)$$

Table 4. Configuration for the experiment

v_b (m/s)	θ	$v_{net(0)}$ (m/s)	X_{ground} (m)	$x_d = D_{init}$ (m)	H_{net} (m)	v_d (m/s)	Δx_2 (cm)
10.0217	15	9.68	4.0436	1	2.2417	4.312	19.0316
				1.5	2.7417	5.3294	23.5224
				2	3.2417	6.1817	27.2839
				2.5	3.7417	6.9299	30.5862
				3	4.2417	7.6048	33.5651
	30	8.68	3.6254	1	2.2289	4.2828	18.9029
				1.5	2.7289	5.3059	23.4184
				2	3.2289	6.1614	27.1943
				2.5	3.7289	6.9118	30.5062
				3	4.2289	7.5883	33.4923
	45	7.09	2.9601	1	2.1963	4.2076	18.5708
				1.5	2.6963	5.2453	23.1512
				2	3.1963	6.1093	26.9645
				2.5	3.6963	6.8654	30.3016
				3	4.1963	7.5461	33.306

4. Results

Table 5. Result of the simulations and experiments

θ	D_{init} (m)	Capture status		Conformity
		Simulation	Experiment	
15	1	Captured	Captured (before full deploy)	v
	1.5	Captured	Captured (before full deploy)	v
	2	Captured	Captured (almost full deployed)	v
	2.5	Captured	Captured (full deployed)	v
	3	Failed	Captured (shrinked)	x
30	1	Captured	Captured (full deployed)	v
	1.5	Captured	Captured (started to shrink)	v
	2	Contacted	Captured (shrinked)	x
	2.5	Failed	Captured (shrinked)	x
	3	Failed	Captured (shrinked and moved to the ground)	x
45	1	Captured	Captured (shrinked)	v
	1.5	Captured	Captured (shrinked)	v
	2	Failed	Captured (shrinked and moved to the ground)	x
	2.5	Not reached	Not reached	v
	3	Not reached	Not reached	v

Influence of θ and D_{init} to net contact and capture condition

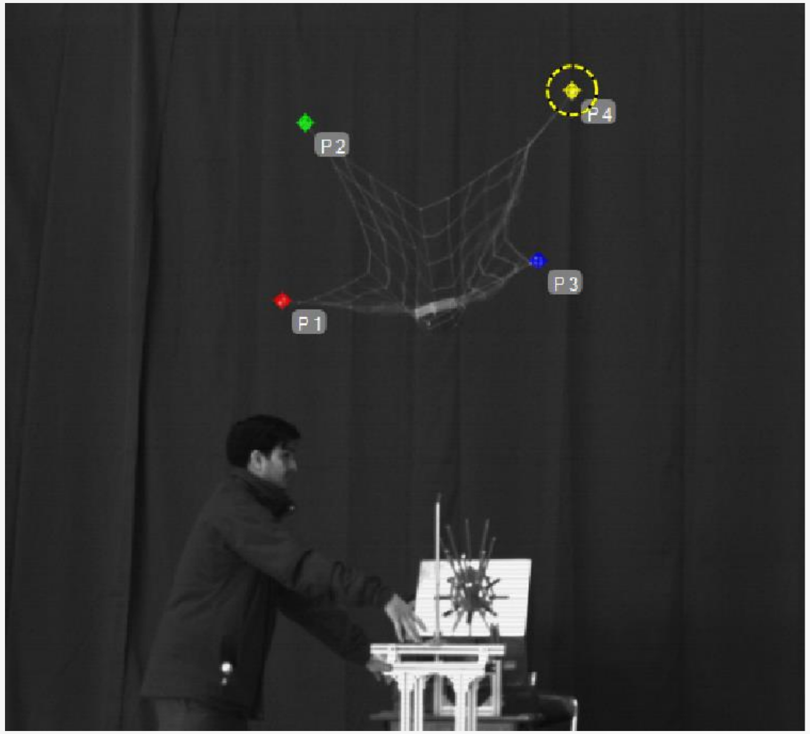

a) Before full deployment

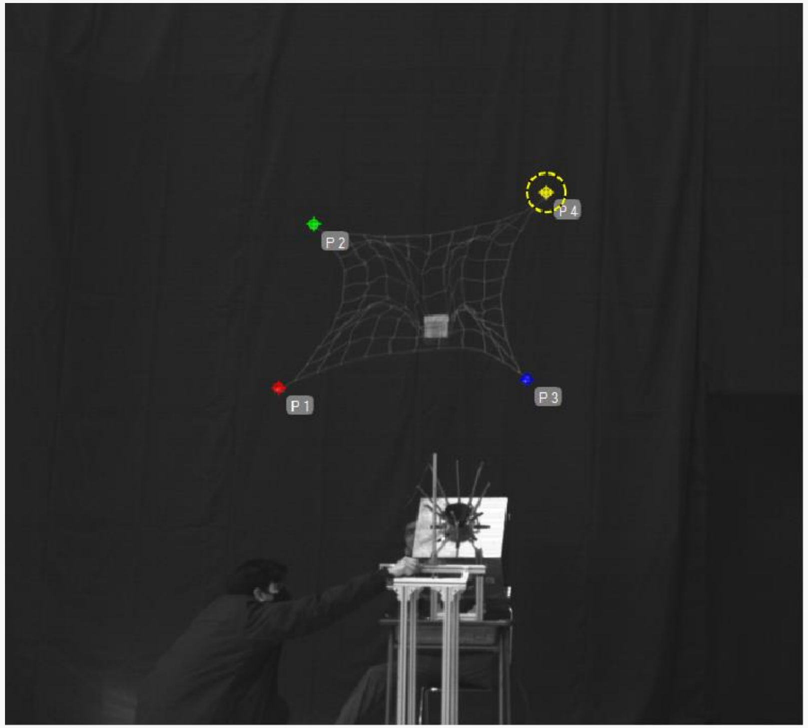

b) Full deployment

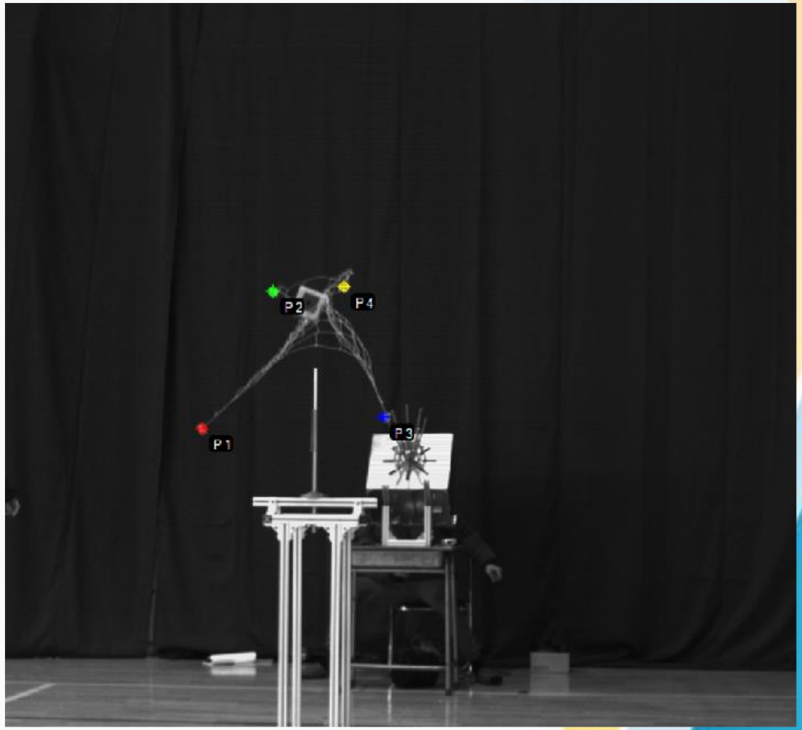

c) Shrinking and closing

Fig. 12 Net condition at the time of contact

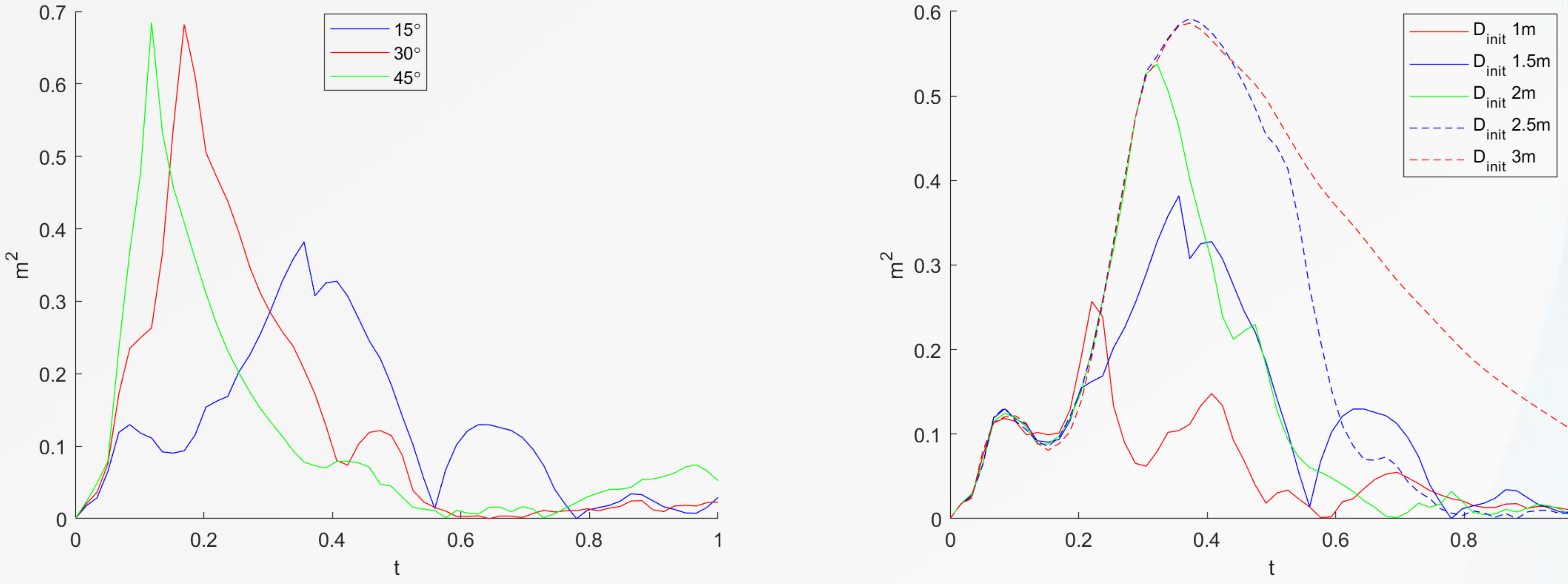

a) Effect of θ (case of D_{init} = 1.5 m)

b) Effect of D_{init} (case of θ = 15°)

Fig. 13 Effect of θ and D_{init} on net deployment

- The larger values of D_{init}, result in the net's broader perimeter opening performance
- On average, the net will reach its peak opening or deployment within 0.4 s after being ejected
- In Figure 13(b), the net's opening should be identical **if unobstructed by D_{init}** .

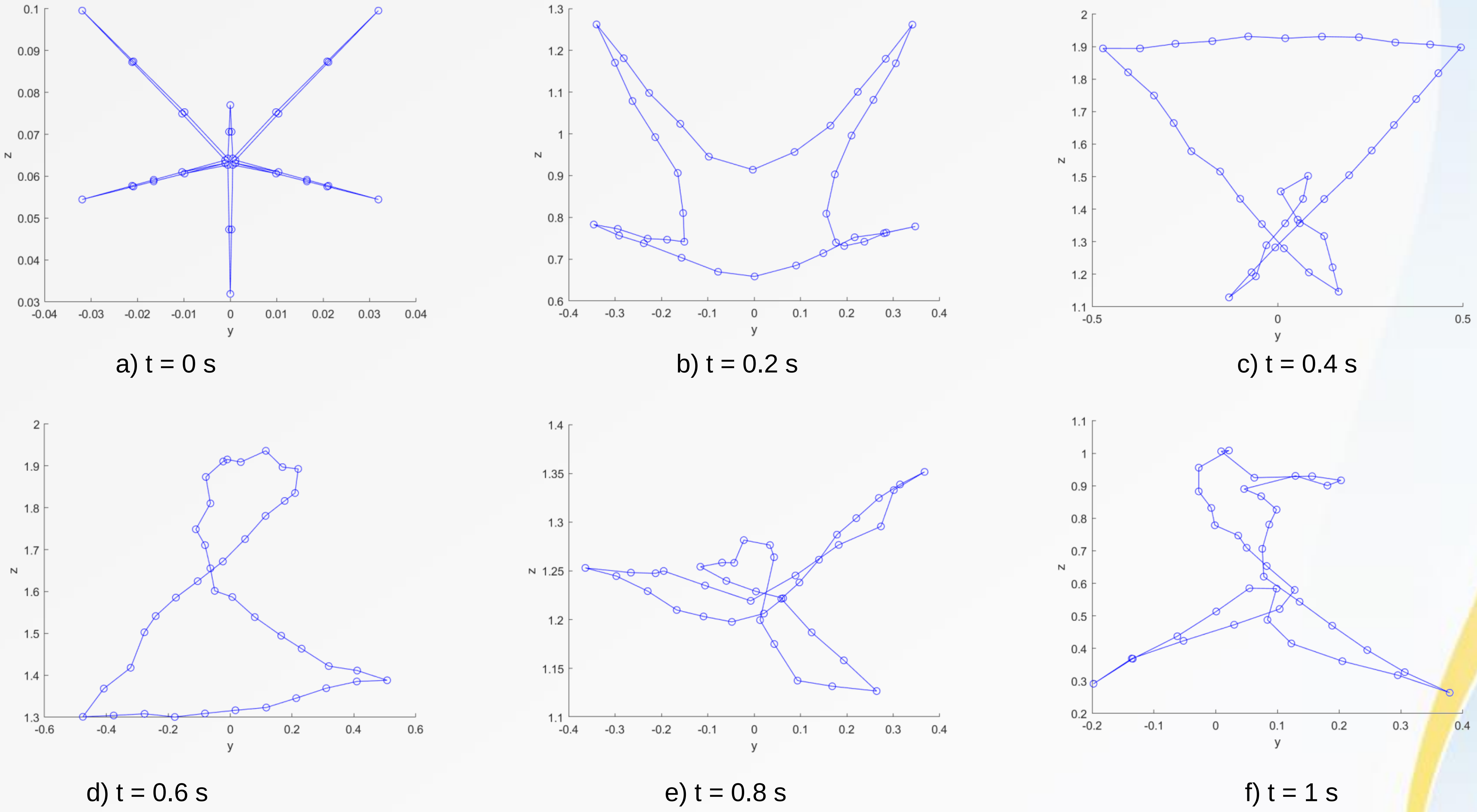

Fig. 14 Sequence of nodes position on the perimeter of net in the simulation (case of D_{init} = 1.5 m and θ = 15°)

Experimental footage processing using HS camera

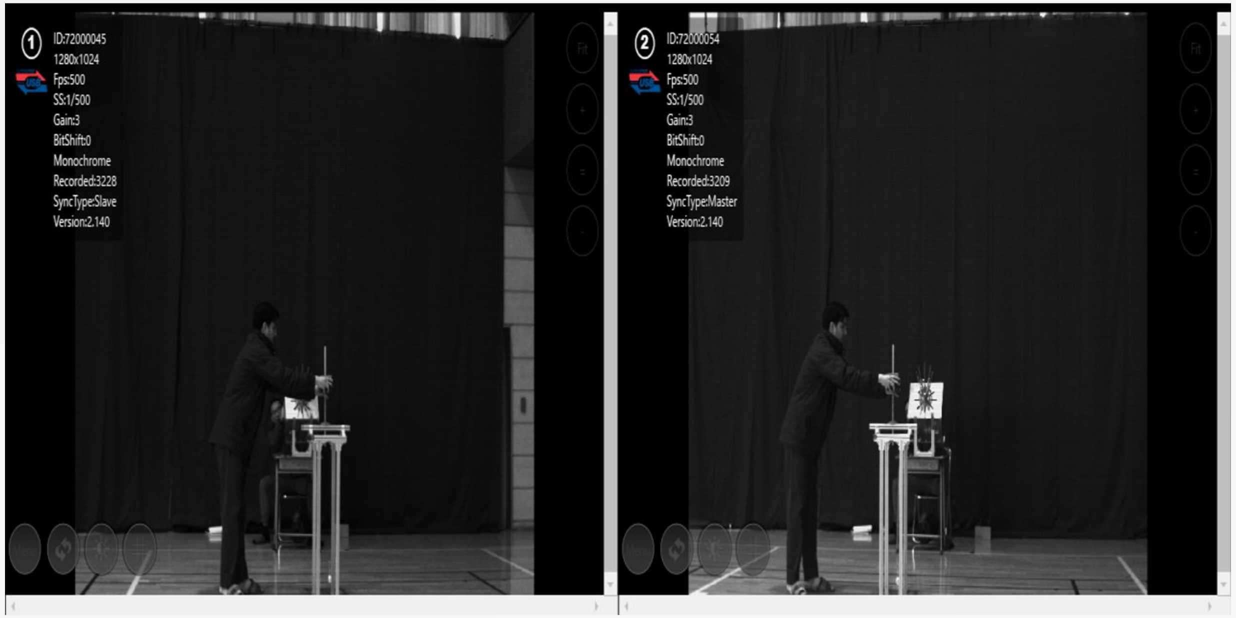

Simulation (time frame 60 fps)

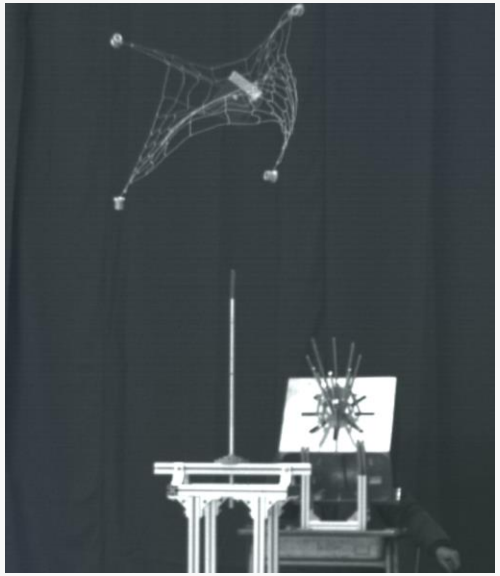

Fig. 15 Contact in case of experiment

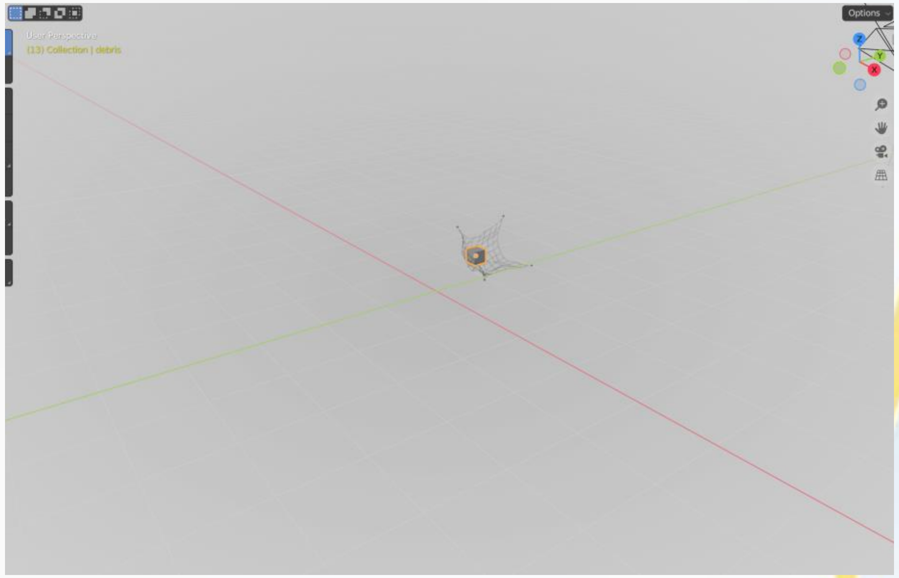

Fig. 16 Contact in case of simulation

Table 6. Net performance

θ	D_{init} (m)	H_{net} (m)	$t_{contact}$ (s)		
			Analytical	Simulation	Experiment
15	1	2.2417	0.2207	0.217	0.26
	1.5	2.7417	0.3584	0.283	0.4
	2	3.2417	0.5236	0.35	0.48
	2.5	3.7417	0.7139	0.5	0.76
	3	4.2417	0.924	0	0.98
30	1	2.2289	0.2227	0.167	0.312
	1.5	2.7289	0.3552	0.25	0.408
	2	3.2289	0.5078	0.367	0.696
	2.5	3.7289	0.6739	0	0.94
	3	4.2289	0.8435	0	1.02
45	1	2.1963	0.2235	0.15	0.46
	1.5	2.6963	0.3423	0.283	0.54
	2	3.1963	0.4651	0	0.78
	2.5	3.6963	0.5793	0	0
	3	4.1963	0.6719	0	0

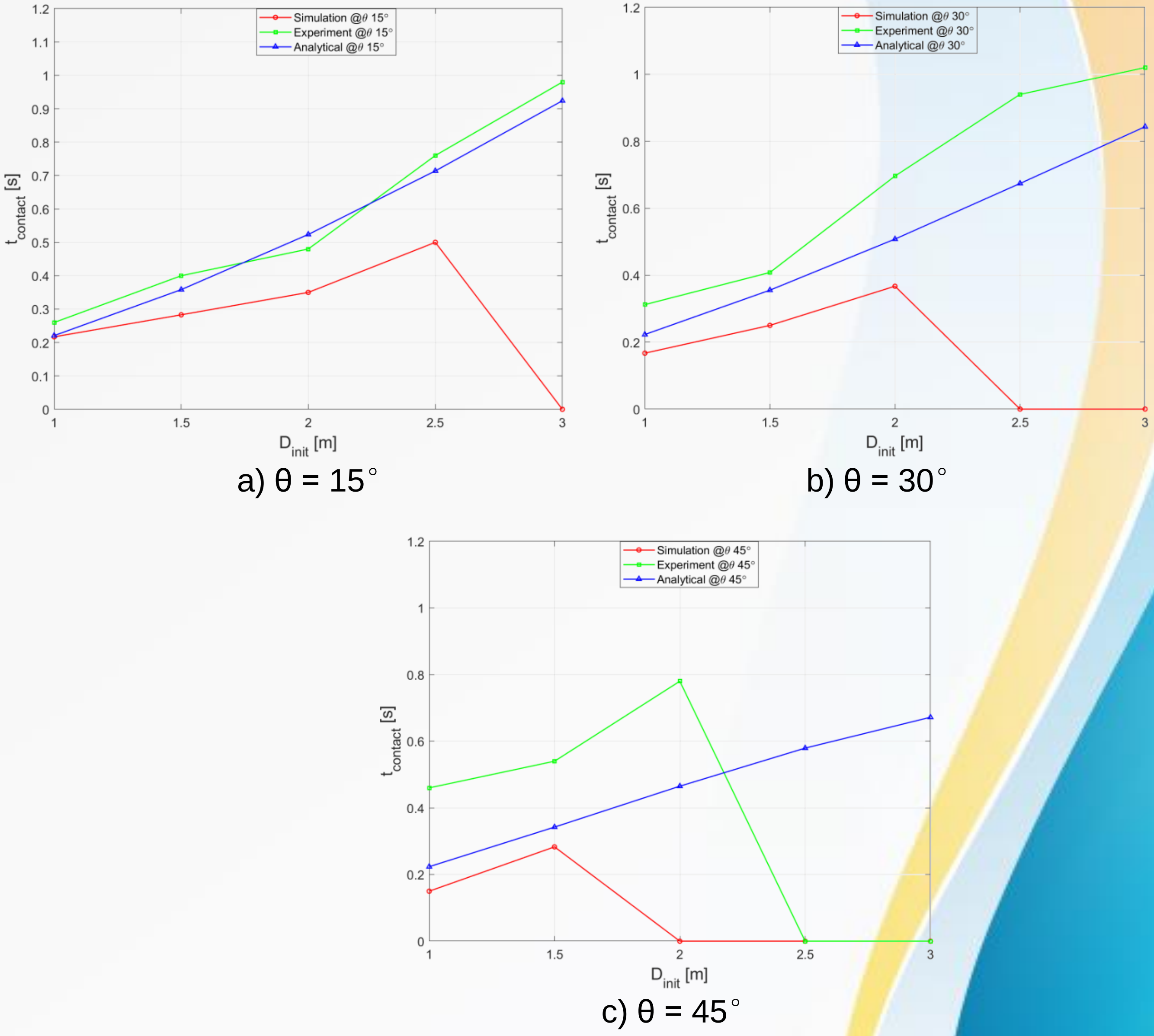

Fig. 17 Comparison of net performance (initial contact time)

Experimental footage processing using HS camera in DippMotion application

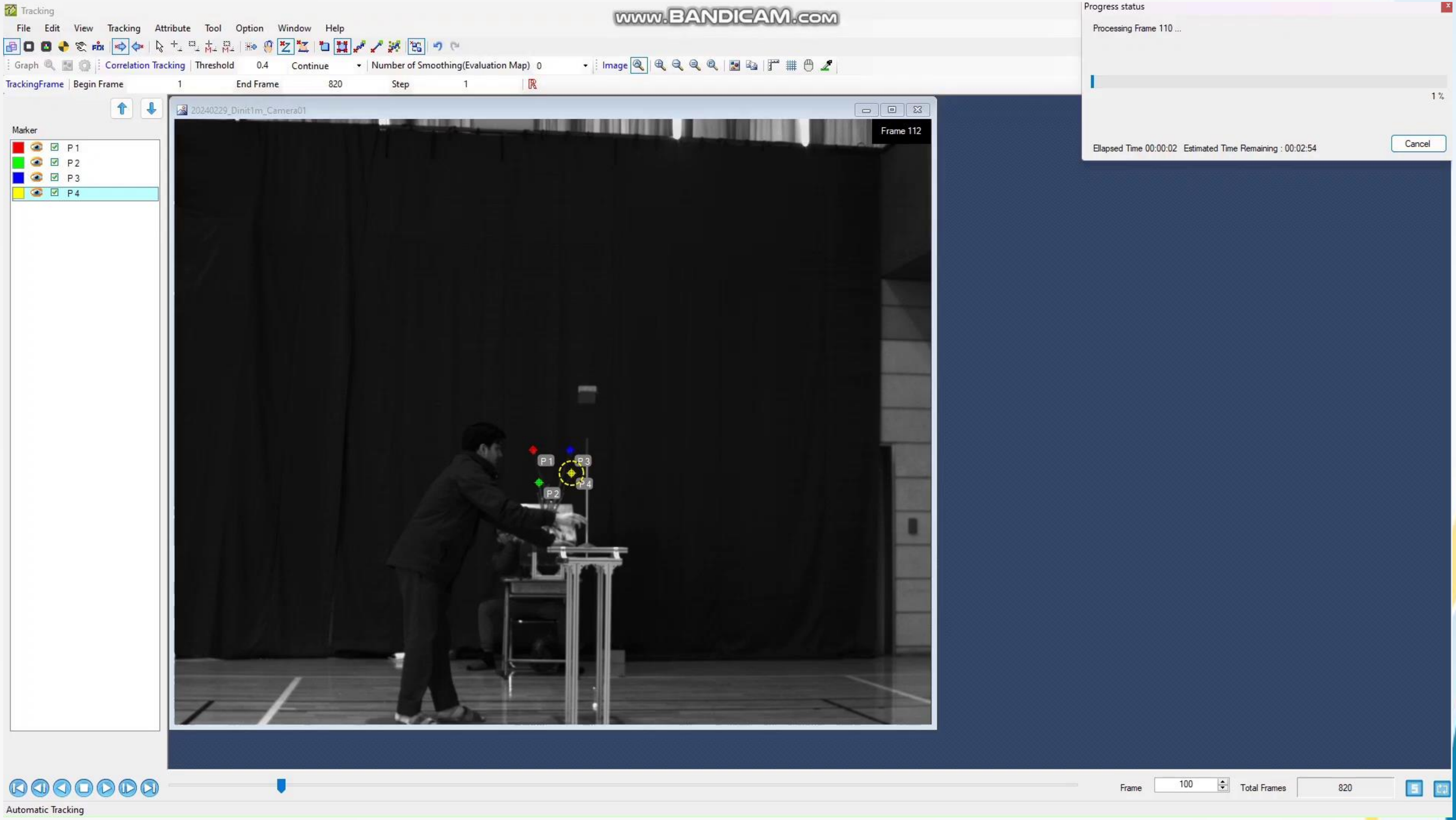

5. Conclusions

1. Impact of net-bullet ejection angles:

- Higher angles widen the net but also cause it to close faster, affecting velocity and reach.
- If the bullet ejection angle increased, then the net opened earlier.

2. Influence of initial distances:

- Larger initial distances widen nets for better debris capture, but reduce net velocity, hindering reach.
- Ideal distances balance net size and speed for maximum capture rates.

Contact and capture can occur at any stage of net deployment—before full opening, during full opening, or as the net starts to shrink— which depends on and is influenced by bullet ejection angle and initial distance.

3. Numerical simulations and ground test:

- Experiments face challenges: timing precision and mechanical constraints.